

# Time-dependent lattice methods for ion-atom collisions in Cartesian and cylindrical coordinate systems

M. S. Pindzola

*Department of Physics, Auburn University, Auburn, Alabama 36849, USA*

D. R. Schultz

*Physics Division, Oak Ridge National Laboratory, Oak Ridge, Tennessee 37831, USA*

(Received 28 September 2007; published 10 January 2008)

Time-dependent lattice methods in both Cartesian and cylindrical coordinates are applied to calculate excitation cross sections for  $p+H$  collisions at 40 keV incident energy. The time-dependent Schrödinger equation is solved using a previously formulated Cartesian coordinate single-channel method on a full 3D lattice and a newly formulated cylindrical coordinate multichannel method on a set of coupled 2D lattices. Cartesian coordinate single-channel and cylindrical coordinate five-channel calculations are found to be in reasonable agreement for excitation cross sections from the  $1s$  ground state to the  $2s$ ,  $2p$ ,  $3s$ ,  $3p$ , and  $3d$  excited states. For extension of the time-dependent lattice method to handle the two electron dynamics found in  $p+He$  collisions, the cylindrical coordinate multichannel method appears promising due to the reduced dimensionality of its lattice.

DOI: [10.1103/PhysRevA.77.014701](https://doi.org/10.1103/PhysRevA.77.014701)

PACS number(s): 34.50.Fa

## I. INTRODUCTION

An accurate treatment of ion-atom collisions remains a computational challenge. From the theoretical point of view, an exact treatment of an ion-atom collision is given through a full solution of the time-dependent Schrödinger equation. Since basis set expansions have their limitations, it has become useful to directly represent the electronic wave function on a numerical lattice. To date such time-dependent lattice methods have been applied to the one electron processes of excitation, ionization, and charge transfer found in  $p+H$  [1–6],  $p+He$  [7],  $p+Li$  [8–10],  $\alpha+H$  [11], and  $Be^{4+}+H$  [12] collisions. All these recent applications are based on representing the electronic wave function on a three-dimensional (3D) Cartesian coordinate lattice.

The application of time-dependent lattice methods to the study of two-electron processes in ion-atom collisions has proved to be a major computational challenge. Recently, a time-dependent multichannel method on a spherical coordinate two-dimensional (2D) lattice was applied to study double ionization processes in  $\alpha+He$  collisions [13]. However, the method is limited to high projectile energies at which all charge-transfer processes are negligible. For intermediate projectile energies at which charge-transfer processes must be included, the application of a six-dimensional (6D) Cartesian coordinate time-dependent lattice has yet to be attempted due to its computational size.

In this paper, we reexamine the use of a cylindrical coordinate time-dependent lattice method to study the one-electron process of excitation in  $p+H$  collisions. Our formulation of the cylindrical coordinate time-dependent lattice method is based on solution in a target frame of reference, as opposed to earlier pioneering work [14] based on solution in a center of mass frame of reference. For identical grid size and spacing, we compare Cartesian and cylindrical coordinate time-dependent lattice calculations for excitation probabilities and cross sections in  $p+H$  collisions at 40 keV in-

cident energy. Our main goal is to check whether the cylindrical coordinate time-dependent 2D lattice calculations with a small number of coupled channels are in reasonable agreement with the Cartesian coordinate 3D lattice calculations. Reasonable agreement would give promise for the formulation and application of a cylindrical coordinate method on a coupled four-dimensional (4D) lattice to address the full range of two-electron processes in ion-atom collisions. The time-dependent lattice methods are presented in Sec. II, the results for excitation from the  $1s$  ground state to the  $2s$ ,  $2p$ ,  $3s$ ,  $3p$ , and  $3d$  excited states in  $p+H$  collisions are presented and discussed in Sec. III, and a brief summary is found in Sec. IV. Atomic units are used throughout unless otherwise indicated.

## II. THEORY

The time-dependent Schrödinger equation for a bare ion projectile colliding with a hydrogenic target atom is given by

$$i \frac{\partial \Psi(\vec{r}_e, t)}{\partial t} = \left( -\frac{1}{2} \nabla^2 - \frac{Z_t}{|\vec{r}_e|} - \frac{Z_p}{|\vec{r}_e - \vec{r}_p(t)|} \right) \Psi(\vec{r}_e, t), \quad (1)$$

where  $Z_t$  is the target atom nuclear charge,  $\vec{r}_e$  is the target electron position vector,  $Z_p$  is the projectile ion nuclear charge, and  $\vec{r}_p(t)$  is the projectile ion position vector.

The total electronic wave function may be directly expressed in Cartesian coordinates as follows:

$$\Psi(\vec{r}_e, t) = P(x, y, z, t). \quad (2)$$

The resulting time-dependent single-channel equation is given by [1]

$$i \frac{\partial P(x, y, z, t)}{\partial t} = T(x, y, z) P(x, y, z, t) + V(x, y, z, t) P(x, y, z, t), \quad (3)$$

where

$$T(x,y,z) = K(x,y,z) - \frac{Z_t}{\sqrt{x^2 + y^2 + z^2}}, \quad (4)$$

$K(x,y,z)$  is the kinetic energy operator, and

$$V(x,y,z,t) = -\frac{Z_p}{\sqrt{(x-b)^2 + y^2 + [z - (z_0 + vt)]^2}}. \quad (5)$$

The projectile follows a straight-line trajectory given by

$$\vec{r}_p(t) = (b, 0, z_0 + vt), \quad (6)$$

where  $b$  is the impact parameter,  $z_0 < 0$  is the starting position, and  $v$  is the velocity.

We solve the time-dependent single-channel equation in Cartesian coordinates using lattice techniques to obtain a discrete representation of the wave function  $P(x,y,z,t)$  and all associated operators on a three-dimensional uniform grid  $(x_i, y_i, z_k)$  [1]. The lowest order finite difference representation of the kinetic energy operator is given by

$$\begin{aligned} K_{i,j,k} P_{i,j,k}(t) = & -\frac{1}{2} \left( \frac{[P_{i+1,j,k}(t) + P_{i-1,j,k}(t) - 2P_{i,j,k}(t)]}{(\Delta x)^2} \right) \\ & -\frac{1}{2} \left( \frac{[P_{i,j+1,k}(t) + P_{i,j-1,k}(t) - 2P_{i,j,k}(t)]}{(\Delta y)^2} \right) \\ & -\frac{1}{2} \left( \frac{[P_{i,j,k+1}(t) + P_{i,j,k-1}(t) - 2P_{i,j,k}(t)]}{(\Delta z)^2} \right). \end{aligned} \quad (7)$$

The total electronic wave function may also be expressed in cylindrical coordinates and expanded in rotational functions as follows:

$$\Psi(\vec{r}_e, t) = \sum_m \frac{P_m(\rho, z, t)}{\sqrt{\rho}} \Phi_m(\phi), \quad (8)$$

where  $\Phi_m(\phi) = \frac{e^{im\phi}}{\sqrt{2\pi}}$ . The resulting time-dependent multichannel equation is given by

$$i \frac{\partial P_m(\rho, z, t)}{\partial t} = T_m(\rho, z) P_m(\rho, z, t) + \sum_{m'} V_{m,m'}(\rho, z, t) P_{m'}(\rho, z, t), \quad (9)$$

where

$$T_m(\rho, z) = K(\rho, z) + \frac{m^2}{2\rho^2} - \frac{Z_t}{\sqrt{\rho^2 + z^2}}, \quad (10)$$

$K(\rho, z)$  is the kinetic energy operator, and

$$\begin{aligned} V_{m,m'}(\rho, z, t) = & -Z_p \sum_{\lambda} \frac{(r_e, r_p)_{\lambda}^{\lambda}}{(r_e, r_p)_{\lambda}^{\lambda+1}} \sum_q \frac{(\lambda - |q|)!}{(\lambda + |q|)!} \\ & \times P_{\lambda}^{|q|}[\cos(\theta_e)] P_{\lambda}^{|q|}[\cos(\theta_p)]. \end{aligned} \quad (11)$$

For the straight-line trajectory of Eq. (6),  $r_e = \sqrt{\rho^2 + z^2}$ ,  $\cos(\theta_e) = \frac{z}{r_e}$ ,  $r_p = \sqrt{b^2 + (z_0 + vt)^2}$ ,  $\cos(\theta_p) = \frac{(z_0 + vt)}{r_p}$ , and  $P_{\lambda}^{|q|}[\cos(\theta)]$  is an associated Legendre function.

We solve the time-dependent multichannel equations in cylindrical coordinates using lattice techniques to obtain a

discrete representation of the wave functions  $P_m(\rho, z, t)$  and all associated operators on a two-dimensional uniform grid. The lowest order finite difference representation of the kinetic energy operator is given by

$$\begin{aligned} K_{i,j} P_{i,j}(t) = & -\frac{1}{2} \left( \frac{[c_i^+ P_{i+1,j}(t) + c_i^- P_{i-1,j}(t) - 2P_{i,j}(t)]}{(\Delta \rho)^2} \right) \\ & -\frac{1}{2} \left( \frac{[P_{i,j+1}(t) + P_{i,j-1}(t) - 2P_{i,j}(t)]}{(\Delta z)^2} \right), \end{aligned} \quad (12)$$

where  $c_i^+ = \frac{\rho_{i+(1/2)}}{\sqrt{\rho_i \rho_{i+1}}}$  and  $c_i^- = \frac{\rho_{i-(1/2)}}{\sqrt{\rho_i \rho_{i-1}}}$ .

For both the Cartesian and cylindrical coordinate methods, a complete set of bound and continuum states for the hydrogenic target atom may be obtained by diagonalizing the Hamiltonian: either  $T(x,y,z)$  or  $T_m(\rho,z)$  for each  $m$ . Alternatively, the lowest energy bound states for the hydrogenic target atom may be found by relaxation of the time-dependent Schrödinger equation for the atom in imaginary time. Schmidt orthogonalization at every time step prevents collapse of excited bound states to lower energy states of the same symmetry.

With the initial condition

$$P(x,y,z,t=0) = P_{1,0}(x,y,z), \quad (13)$$

or

$$P_m(\rho, z, t=0) = P_{1,0}(\rho, z) \Phi_0(\phi) \delta_{m,0}, \quad (14)$$

the time-dependent equations are propagated forward in time using an explicit algorithm given by

$$P(t + \Delta t) = -2i\Delta t H(t) P(t) + P(t - \Delta t), \quad (15)$$

where  $H(t)$  is the full time-dependent Hamiltonian. Following the time propagation of the projectile past the target, excitation probabilities for a given projectile velocity and impact parameter are given by

$$\mathcal{P}_{nlm}(v, b) = \left| \int d\vec{r}_e \Psi_{nlm}^*(\vec{r}_e) \Psi(\vec{r}_e, t \rightarrow \infty) \right|^2, \quad (16)$$

while excitation cross sections for a given projectile velocity are given by

$$\sigma_{nlm}(v) = 2\pi \int_0^{\infty} b db \mathcal{P}_{nlm}(v, b). \quad (17)$$

### III. RESULTS

The Cartesian coordinate single-channel calculations for proton-impact excitation of hydrogen employ a ( $n_x=320$ ,  $n_y=160$ ,  $n_z=320$ ) point lattice. The  $x$  and  $z$  coordinates from  $-32.0$  to  $+32.0$  are spanned by a uniform mesh spacing of  $\Delta x = \Delta z = 0.2$  and the  $y$  coordinate from  $0.0$  to  $32.0$  is spanned by a uniform mesh spacing of  $\Delta y = 0.2$ . Each coordinate mesh is partitioned over  $N_c$  parallel processors. After each time step the wave function at the initial and final points of the partitioned coordinate mesh is passed to its nearest neighbor processor so that the second derivative in the kinetic

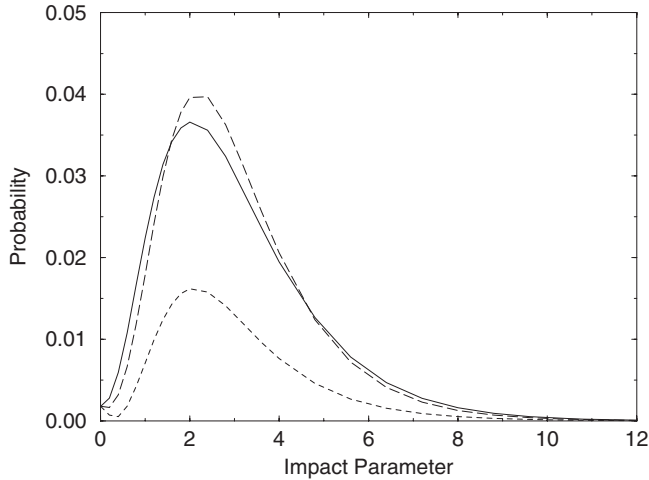


FIG. 1. Proton-impact  $1s \rightarrow 2p$  excitation of hydrogen at 40 keV incident energy. Solid curve: Cartesian coordinate single-channel method. Short-dashed curve: cylindrical coordinate single-channel ( $\lambda_{\max}=3$ ) method. Long-dashed curve: cylindrical coordinate five-channel ( $\lambda_{\max}=3$ ) method (impact parameter in atomic units).

energy may be calculated. In addition, each time-dependent calculation is further partitioned over each impact parameter needed to calculate the cross section. Thus, the total number of parallel processors needed for a given incident energy is  $N_c^3 N_b$ , where  $N_b$  is the number of impact parameters.

The proton projectile begins its journey towards the hydrogen atom in its ground state at an initial position of  $z_0 = -16.0$ . The time-dependent single-channel equation [Eq. (3)] is propagated so that the projectile reaches a final position of  $z = +47.5$ . Spurious wave reflection at the lattice boundary is eliminated through the use of exponential masking. For an incident energy of 40 keV, the  $1s \rightarrow 2p$  and  $1s \rightarrow 3d$  excitation probabilities as a function of impact parameter  $b$  are shown as the solid lines in Figs. 1 and 2. Excitation cross sections from the  $1s$  ground state to the  $2s$ ,  $2p$ ,  $3s$ ,  $3p$ , and  $3d$  excited states are presented in row 6 of Table I. The Cartesian coordinate single-channel excitation cross sections at 40 keV incident energy found in Table I agree reasonably well with previous single center—atomic

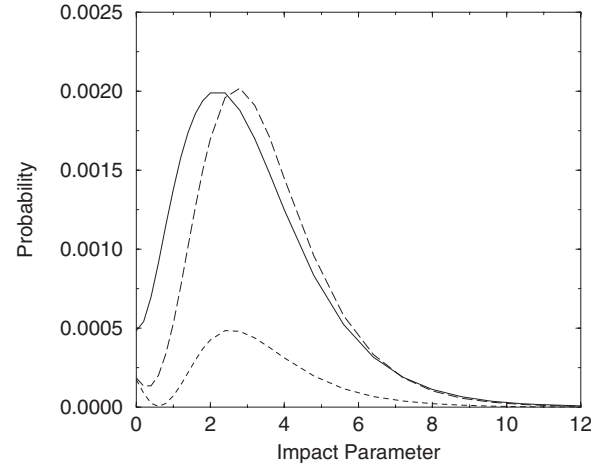


FIG. 2. Proton-impact  $1s \rightarrow 3d$  excitation of hydrogen at 40 keV incident energy. Solid curve: Cartesian coordinate single-channel method. Short-dashed curve: cylindrical coordinate single-channel ( $\lambda_{\max}=3$ ) method. Long-dashed curve: cylindrical coordinate five-channel ( $\lambda_{\max}=3$ ) method (impact parameter in atomic units).

orbital close coupling (SC-AOCC) [15], two center—atomic orbital close coupling (TC-AOCC) [16], lattice time-dependent Schrödinger equation—finite difference (LTDSE-FD) [1], lattice time-dependent Schrödinger equation—Fourier collocation (LTDSE-FC) [3], and two center momentum space discretization (TCMSD) [17] results.

The cylindrical coordinate multichannel calculations for proton-impact excitation of hydrogen employ a ( $n_\rho=160$ ,  $n_z=320$ ) point lattice. The  $\rho$  coordinate from 0.0 to 32.0 is spanned by a uniform mesh spacing of  $\Delta\rho=0.2$  and the  $z$  coordinate from  $-32.0$  to  $+32.0$  is spanned by a uniform mesh spacing of  $\Delta z=0$ . The calculations are again partitioned over each coordinate and impact parameter. The total number of parallel processors needed for a given incident energy is  $N_c^2 N_b$ .

The proton projectile is again propagated from  $z_0 = -16.0$  to  $z = +47.5$ . For an incident energy of 40 keV, the  $1s \rightarrow 2p$  and  $1s \rightarrow 3d$  excitation probabilities as a function of impact parameter  $b$  are shown as the dashed lines in Figs. 1 and 2. The short-dashed lines in Figs. 1 and 2 are from cylindrical

TABLE I. Proton-impact excitation of hydrogen at 40 keV incident energy. Cross sections in units of  $1.0 \times 10^{-18} \text{ cm}^2$ . (cc: coupled channels.)

Method	$1s \rightarrow 2s$	$1s \rightarrow 2p$	$1s \rightarrow 3s$	$1s \rightarrow 3p$	$1s \rightarrow 3d$
SC-AOCC [15]	17.7	68.7	3.9	10.9	3.3
TC-AOCC [16]	17.4	72.0	3.8	12.0	3.4
LTDSE-FD [1]	16.1	76.2	3.5	12.6	4.9
LTDSE-FC [3]	18.5	80.0	3.4	10.5	4.1
TCMSD [17]	15.7	62.7			
Cartesian	16.3	72.4	3.8	12.2	4.5
Cylindrical 1 cc ( $\lambda_{\max}=3$ )	20.2	28.2	6.9	4.2	1.0
Cylindrical 5 cc ( $\lambda_{\max}=3$ )	18.0	72.6	5.3	16.1	4.6
Cylindrical 5 cc ( $\lambda_{\max}=4$ )	16.4	70.8	4.7	15.4	4.6
Cylindrical 5 cc ( $\lambda_{\max}=5$ )	16.0	70.5	4.6	15.4	4.7

coordinate single-channel calculations with  $m=0$  only in Eq. (9). The time-dependent interaction operator of Eq. (11) includes monopole, dipole, quadrupole, and octopole terms, i.e.,  $\lambda_{max}=3$ . The long-dashed lines in Figs. 1 and 2 are from cylindrical coordinate five-channel calculations with  $m=0, 1, -1, 2, -2$  in Eq. (9) and  $\lambda_{max}=3$  in Eq. (11). The Cartesian coordinate single-channel and cylindrical coordinate five-channel ( $\lambda_{max}=3$ ) calculations are in good agreement for all impact parameters, except those close to zero. Since the cross sections are proportional to the impact parameter times the probability in Eq. (17), the discrepancies at small impact parameters have a minimal effect on the agreement between cross sections. Additional cylindrical coordinate five-channel calculations with  $\lambda_{max}=4$  and  $\lambda_{max}=5$  were also carried out. Excitation cross sections from the  $1s$  ground state to the  $2s$ ,  $2p$ ,  $3s$ ,  $3p$ , and  $3d$  excited states are presented in rows 7–10 of Table I. The Cartesian coordinate single-channel and cylindrical coordinate five-channel calculations are found to be in reasonable agreement for all transitions.

#### IV. SUMMARY

Time-dependent lattice methods were applied to calculate excitation cross sections for  $p+H$  collisions at 40 keV inci-

dent energy. The time-dependent Schrödinger equation was solved using both a previously formulated Cartesian coordinate 3D lattice method and a newly formulated cylindrical coordinate coupled 2D lattice method. Calculations using both methods were found to be in reasonable agreement for excitation cross sections from the  $1s$  ground state to the  $2s$ ,  $2p$ ,  $3s$ ,  $3p$ , and  $3d$  excited states.

Based on our excitation calculations, the cylindrical coordinate method on a coupled 2D lattice appears promising for accurately describing heavy particle collisions with atoms involving other one-electron processes. Our next step is to develop the computational tools needed to extract single charge-transfer cross sections using the cylindrical coordinate method. If all goes well, an extension of the cylindrical coordinate method from a coupled 2D lattice to a coupled 4D lattice could then be made for accurately describing heavy particle collisions with atoms involving fully correlated two-electron dynamics.

#### ACKNOWLEDGMENTS

This work was supported in part by grants from the U.S. Department of Energy. Computational work was carried out at the National Energy Research Scientific Computing Center in Oakland, California.

- 
- [1] A. Kolakowska, M. S. Pindzola, F. Robicheaux, D. R. Schultz, and J. C. Wells, Phys. Rev. A **58**, 2872 (1998).
  - [2] A. Kolakowska, M. S. Pindzola, and D. R. Schultz, Phys. Rev. A **59**, 3588 (1999).
  - [3] D. R. Schultz, M. R. Strayer, and J. C. Wells, Phys. Rev. Lett. **82**, 3976 (1999).
  - [4] D. R. Schultz, C. O. Reinhold, P. S. Krstic, and M. R. Strayer, Phys. Rev. A **65**, 052722 (2002).
  - [5] M. Chassid and M. Horbatsch, Phys. Rev. A **66**, 012714 (2002).
  - [6] M. S. Pindzola, T. G. Lee, T. Minami, and D. R. Schultz, Phys. Rev. A **72**, 062703 (2005).
  - [7] T. Minami, C. O. Reinhold, D. R. Schultz, and M. S. Pindzola, J. Phys. B **37**, 4025 (2004).
  - [8] M. S. Pindzola, Phys. Rev. A **60**, 3764 (1999).
  - [9] M. S. Pindzola, Phys. Rev. A **66**, 032716 (2002).
  - [10] M. S. Pindzola, T. Minami, and D. R. Schultz, Phys. Rev. A **68**, 013404 (2003).
  - [11] M. E. Riley and B. Ritchie, Phys. Rev. A **59**, 3544 (1999).
  - [12] T. Minami, M. S. Pindzola, T. G. Lee, and D. R. Schultz, J. Phys. B **39**, 2877 (2006).
  - [13] M. S. Pindzola, F. Robicheaux, and J. Colgan, J. Phys. B **40**, 1695 (2007).
  - [14] N. Grun, A. Muhlaus, and W. Scheid, J. Phys. B **15**, 4043 (1982).
  - [15] A. L. Ford, J. F. Reading, and K. A. Hall, J. Phys. B **26**, 4537 (1993).
  - [16] J. Kuang and C. D. Lin, J. Phys. B **29**, 5443 (1996).
  - [17] E. Y. Sidky and C. D. Lin, Phys. Rev. A **65**, 012711 (2001).